Ray tracing and refraction in the modified US1976 atmosphere

Siebren Y. van der Werf

A new and flexible ray-tracing procedure for calculating astronomical refraction is outlined and applied to the US1976 standard atmosphere. This atmosphere is generalized to allow for a free choice of the temperature and pressure at sea level, and in this form it has been named the modified US1976 (MUSA76) atmosphere. Analytical expressions and numerical procedures are presented for calculating dry-air refractions and for the water-vapor correction. Results for all apparent altitudes are presented and compared with *The Star Almanac for Land Surveyors* (1951), *The Nautical Almanac* (1958), and the Pulkovo tables (*Refraction Tables of the Pulkovo Observatory*, 1985). Dependences on sea-level pressure, temperature, and temperature gradient and on humidity are discussed.

OCIS codes: 010.1290, 010.4030, 010.7030.

1. Introduction

Refraction has intrigued mankind for the past two millennia. Computations on the basis of atmospheric models are numerous, both in approximative closed form and, in this computer era, by ray tracing. The atmospheric models that underlie some commonly used tabulations, such as *The Star Almanac for Land Surveyors*[1] and *The Nautical Almanac*,[2] are, however, of relatively old age. The more modern U.S. standard atmosphere of 1976,[3] adopted in the meteorological world, has not yet found its way into widely used tables. We discuss in this study an adapted form of it: the modified US1976 atmosphere or MUSA76. It is generalized in such a way that sea-level pressure and temperature have been made adjustable and the effect of humidity may be incorporated.

In earlier research[4] analytical expressions for the dry-air pressure and the water-vapor correction have been given, derived under the assumption of a constant acceleration of gravity. In the US1976 atmosphere the acceleration of gravity depends on height, and we present new analytical expressions for the partial dry-air and water-vapor pressures. In addition, we present methods for numerical evaluation.

We derive a scaling law for dry-air MUSA76 refractions that relates refractions at different sea-level temperature and pressure, and this is compared with direct calculations.

A full ray-tracing procedure, for well-behaved temperature profiles equivalent to the common Auer–Standish[5] refraction integral formulation, but more flexible for nonstandard atmospheres, is presented in detail.

Comparisons with the *Star Almanac*[1] and the *Nautical Almanac*[2] are made for the sea-level pressures and temperatures for which they have been defined, and an additional comparison is made with the more modern Pulkovo tables.[6]

2. Ray Tracing

The curvature of a path is given by the inverse of the local radius of curvature, r. With reference to Fig. 1, and introducing polar coordinates as $x = R\sin(\phi)$, $y = R\cos(\phi)$ and $R = R(\phi)$, the curvature reads

$$\frac{1}{r} = \frac{\dfrac{\mathrm{d}^2 y}{\mathrm{d}x^2}}{\left[1 + \left(\dfrac{\mathrm{d}y}{\mathrm{d}x}\right)^2\right]^{3/2}} = \frac{-R^2 + R\,\dfrac{\mathrm{d}^2 R}{\mathrm{d}\phi^2} - 2\left(\dfrac{\mathrm{d}R}{\mathrm{d}\phi}\right)^2}{\left[R^2 + \left(\dfrac{\mathrm{d}R}{\mathrm{d}\phi}\right)^2\right]^{3/2}}. \tag{1}$$

Denoting in any point of the path the angle between the local tangent and the circle around the

S. Y. van der Werf (vdwerf@kvi.nl) is with the Kernfysisch Versneller Instituut, University of Groningen, Zernikelaan 25, 9747 AA Groningen, The Netherlands.

Received 10 December 2001; revised manuscript received 21 March 2002.

0003-6935/03/030354-13$15.00/0

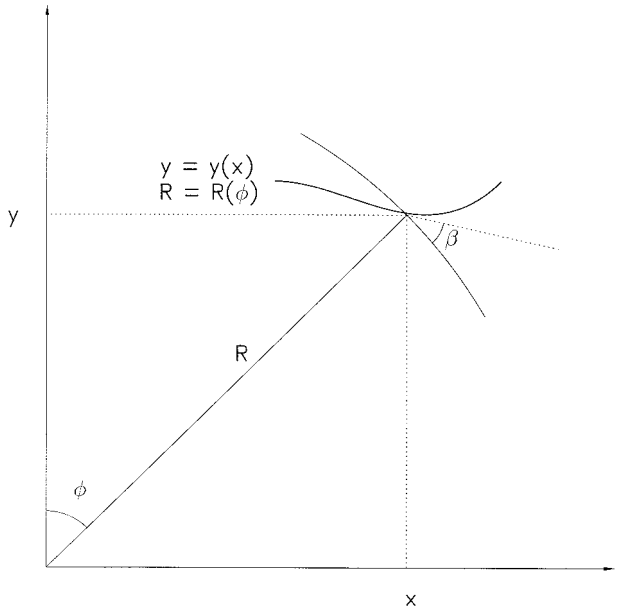

Fig. 1. Arbitrary path in Cartesian coordinates and in the spherical coordinates R, ϕ, and β, on which the ray-tracing method is based.

origin that passes through the same point, as β, one has

$$\beta = \arctan\left(\frac{1}{R}\frac{\mathrm{d}R}{\mathrm{d}\phi}\right), \tag{2}$$

$$\frac{\mathrm{d}\beta}{\mathrm{d}\phi} = \frac{-R^2 + R\,\dfrac{\mathrm{d}^2R}{\mathrm{d}\phi^2} - 2\left(\dfrac{\mathrm{d}R}{\mathrm{d}\phi}\right)^2}{\left[R^2 + \left(\dfrac{\mathrm{d}R}{\mathrm{d}\phi}\right)^2\right]} + 1. \tag{3}$$

The denominator of the above equation can be rewritten as

$$\left[R^2 + \left(\frac{\mathrm{d}R}{\mathrm{d}\phi}\right)^2\right]^{1/2} = R[1 + \tan^2(\beta)]^{1/2} = R/\cos(\beta), \tag{4}$$

and from Eqs. (1)–(3) follows

$$\frac{\mathrm{d}R}{\mathrm{d}\phi} = R\,\tan(\beta), \tag{5}$$

$$\frac{\mathrm{d}\beta}{\mathrm{d}\phi} = 1 + \frac{1}{r}\frac{R}{\cos(\beta)}. \tag{6}$$

These are two coupled first-order differential equations for R and β with ϕ as a common variable. This scheme can be solved by standard numerical integration techniques if $r = r(R, \beta, \phi)$ can be evaluated in any point.

When this is specialized to the Earth's atmosphere, the curvature of a light path can be related to the index of refraction. For a spherically symmetric atmosphere a well-known law, to be found in many textbooks,[7,8] states

$$nR\,\cos(\beta) = \text{constant}, \tag{7}$$

whence one obtains, by expanding to first order in differentials and upon dividing by $\mathrm{d}\phi$,

$$\tan(\beta)\,\frac{\mathrm{d}\beta}{\mathrm{d}\phi} = \left(\frac{1}{R} + \frac{1}{n}\frac{\mathrm{d}n}{\mathrm{d}R}\right)\frac{\mathrm{d}R}{\mathrm{d}\phi}. \tag{8}$$

Using Eq. (5), one obtains

$$\frac{\mathrm{d}\beta}{\mathrm{d}\phi} - 1 = \frac{R}{n}\frac{\mathrm{d}n}{\mathrm{d}R}, \tag{9}$$

and comparing this with Eq. (6) gives

$$\frac{1}{r} = \cos(\beta)\,\frac{1}{n}\frac{\mathrm{d}n}{\mathrm{d}R}. \tag{10}$$

More generally and more concisely this result may be written as[7]

$$\frac{1}{r} = \frac{1}{n}\,\hat{\nu}\,\cdot\,\nabla n, \tag{11}$$

where $\hat{\nu}$ is an, *ad hoc* introduced, unit vector perpendicular to the direction of the light ray.

Alternatively, and more physically, one may write

$$\frac{\hat{\mathbf{r}}}{|\mathbf{r}|} = \hat{\mathbf{k}} \times \frac{1}{n}\,\nabla n, \tag{12}$$

where $\hat{\mathbf{k}}$ is the direction of the light ray and the unit vector $\hat{\mathbf{r}}$ gives the direction in which the light is deflected via the right-hand rule of the vector product; i.e., the tip of the $\hat{\mathbf{k}}$ vector is deflected into the direction $-\hat{\mathbf{k}} \times [\hat{\mathbf{k}} \times (1/n)\nabla n]$.

Hence, the system of coupled differential equations, Eqs. (5) and (6), reads as

$$\frac{\mathrm{d}R}{\mathrm{d}\phi} = R\,\tan(\beta), \tag{13}$$

$$\frac{\mathrm{d}\beta}{\mathrm{d}\phi} = 1 + \frac{R}{n}\frac{\mathrm{d}n}{\mathrm{d}R}. \tag{14}$$

Results discussed in this paper are obtained by solving these equations by fourth-order Runge–Kutta integration, following the light path from the height of the observer to the edge of the stratosphere, which is put at 85 km. The total refraction is obtained as

$$\xi = \int_{\text{Path}} (\mathrm{d}\beta - \mathrm{d}\phi). \tag{15}$$

Another approach is to rewrite Eq. (15) as

$$\xi = \int_{\beta_0}^{\beta_s}\left(1 - \frac{\mathrm{d}\phi}{\mathrm{d}\beta}\right)\mathrm{d}\beta = \int_{\beta_0}^{\beta_s}\frac{R\mathrm{d}n/\mathrm{d}h}{n + R\mathrm{d}n/\mathrm{d}h}\,\mathrm{d}\beta, \tag{16}$$

where the integration limits β_0, the apparent altitude for the observer, and β_s, the value at the edge of the stratosphere are obtained directly from Eq. (7). This is the refraction integral as proposed by Auer and Standish,[5] and it is widely used in this form.[4,9,10] The integrand of Eq. (16) is then evaluated for discrete equidistant values of β, and the integral is numerically performed, e.g., by Simpson integration.

At first sight it looks as if explicit ray tracing is avoided here. But for a practical evaluation of the refraction integral it is necessary to construct a lookup table of values of the product $n(h)(R_{\mathrm{Earth}} + h)$ versus h, from which h can be found for each value of β, e.g., by Newton–Raphson iteration. Hence, the information on height, h, is preserved. On the other hand, the information on horizontal distance, embodied in the parameter ϕ, is not taken along.

Of course both methods do give identical results, and the choice between one or the other is a matter of taste. We find full ray tracing, using Runge–Kutta integration, the more flexible method, as it allows more easily for generalizations of the atmosphere. In particular, temperature profiles may be such that the product $n(h)(R_{\mathrm{Earth}} + h)$ is no longer a monotonic function of h. Also, the characteristics of the atmosphere may change with distance along the Earth's surface so that it is no longer spherically symmetrical. These circumstances may occur in the presence of strong temperature inversions. In such cases, ray tracing can still be done, but the refraction integral approach can no longer be used. The necessary extensions of the ray-tracing procedure are discussed in two other papers in this issue, which deal with the Novaya Zemlya effect.[11,12]

3. Index of Refraction in the MUSA76 Atmosphere

The atmosphere is considered to be made up of two ideal gases, dry air and water vapor, with molecular masses m_D and m_W, respectively. Given a temperature profile, $T(h)$, the total pressure must be found from the differential equation

$$\frac{\mathrm{d}P}{\mathrm{d}h} = \frac{\mathrm{d}P_D}{\mathrm{d}h} + \frac{\mathrm{d}P_W}{\mathrm{d}h} = -\frac{m_D g(h)}{k}\frac{P_D(h)}{T(h)} - \frac{m_W g(h)}{k}\frac{P_W(h)}{T(h)}, \quad (17)$$

where k is Boltzmann's constant. The acceleration of gravity varies with height as

$$g(h) = g(0)\left(\frac{R_{\mathrm{Earth}}}{R_{\mathrm{Earth}} + h}\right)^2. \quad (18)$$

For the temperature profile we adopt the US1976 atmosphere, modified in the troposphere to allow for a free choice of the temperature at ground or sea level. This temperature profile is characterized by piecewise constant temperature gradients. Atmospheres that are obtained by slight variations of the US1976 parameters have been considered by Sampson[13] and have been named modified US1976 standard atmospheres (MUSSAs). We shall use one particular modification, namely, that we make the sea-level pressure, P_0, and the sea-level temperature, T_0, adjustable. In this form, explained in Table 1, we denote the so modified US1976 atmosphere as MUSA76. We adopt the values for natural and geophysical constants from the latest *Handbook of Chemistry and Physics*[3]:

Table 1. MUSA76 Atmosphere[a]

h_1 (km)	h_2 (km)	$\mathrm{d}T/\mathrm{d}h$ (K/km)	$T(h_1)$ (K)
0	H_T[a]	−6.5	T_0
H_T[a]	20	0.0	216.65
20	32	1.0	216.65
32	47	2.8	228.65
47	51	0.0	270.65
51	71	−2.8	270.65
71	85	−2.0	214.65

[a] P_0 and T_0 are adjustable. $H_T = (T_0 - 216.65)/6.5$ km. Standard values of US1976: $P_0 = 1013.25$ hPa, $T_0 = 288.15$ K, $H_T = 11$ km.

N = Avogadro's number,

$R = Nk = 8314.472\ \mathrm{J\ kmol^{-1}\ K^{-1}}$ (universal gas constant),

$M_D = Nm_D = 28.964$ kg (mass per kmol of dry air),

$M_D = Nm_W = 18.016$ kg (mass per kmol of water vapor),

$R_E = 6356766$ m (the Earth's mean radius at 45 °N),

$g(0) = 9.780356[1 + 0.0052885\ \sin^2(\phi) - 0.0000059\ \sin^2(2\phi)]\ \mathrm{m/s^2}$ (ϕ = latitude),

Once the pressures have been evaluated, the index of refraction follows from

$$n_\lambda(h) - 1 = \frac{1}{T(h)}[A_D(\lambda)P_D(h) + A_W(\lambda)P_W(h)]. \quad (19)$$

We name A_D and A_W the reduced refractivities of dry air and water. They are expressed in $\mathrm{hPa^{-1}\ K}$. The *Handbook of Chemistry and Physics* gives $A_D(\lambda)$ in Edlen's[14] first-order approach to Sellmeier's form:

$$A_D(\lambda) = 10^{-8}[8342.13 + 2406030(130 - 1/\lambda^2)^{-1} + 15997(38.9 - 1/\lambda^2)^{-1}]\frac{288.15}{1013.25}, \quad (20)$$

where λ is given in micrometers. A more recent expression has been given by Ciddor[15]:

$$A_D(\lambda) = 10^{-8}[5792105(238.0185 - 1/\lambda^2)^{-1} + 1167917(57.362 - 1/\lambda^2)^{-1}]\frac{288.15}{1013.25}. \quad (21)$$

Of interest here is also the version used in the *Explanatory Supplement to the Astronomical Almanac* and by Hohenkerk and Sinclair,[4,9,10] which uses the Cauchy form:

$$A_D(\lambda) = 10^{-8}\left[28760.4 + \frac{162.88}{\lambda^2} + \frac{1.36}{\lambda^4}\right]\frac{273.15}{1013.25}. \quad (22)$$

In the range of visible light these three expressions give reduced refractivities that agree at the level of 1 part in 10^4, and the ray-tracing results that will be presented in later sections depend only very slightly upon the choice for one or the other. We shall adopt the form of Ciddor for our MUSA76 calculations but make a comparison with the Cauchy form in the case of the *Star Almanac*.

The reduced refractivity for water A_W is less precisely known. In the *Explanatory Supplement*, Hohenkerk and Sinclair[4,9,10] adopt

$$A_W(\lambda) = 10^{-8}\left[24580.4 + \frac{162.88}{\lambda^2} + \frac{1.36}{\lambda^4}\right]\frac{273.15}{1013.25}. \quad (23)$$

Recently, Ciddor[15] found, by scaling an expression of Owen[16] to fit modern measured values,

$$A_W(\lambda) = 1.022 \times 10^{-8}\left[295.235 + \frac{2.6422}{\lambda^2} - \frac{0.032380}{\lambda^4} + \frac{0.004028}{\lambda^6}\right]\frac{293.15}{13.33}. \quad (24)$$

These expressions give reduced refractivities that differ by 1%. We adopt Ciddor's form for our MUSA76 calculations but shall compare the two expressions when studying the *Star Almanac* atmosphere.

4. Calculation of the Dry-Air and Water-Vapor Pressures

The water-vapor pressure depends explicitly only on temperature, and Eq. (17) is rewritten as

$$\frac{dP_D}{dh} + \frac{m_D g(h)}{k}\frac{P_D(h)}{T(h)} = -\frac{dP_W(T)}{dT}\frac{dT}{dh} - \frac{m_W g(h)}{k}\frac{P_W[T(h)]}{T(h)}. \quad (25)$$

For dry air, $P_W = 0$ and the right-hand side vanishes. We shall follow the lines of the *Explanatory Supplement*[4] and allow for a water-vapor contribution only in the troposphere. The relative humidity, RH, is taken constant right up to the tropopause. The water-vapor pressure depends then not explicitly on height, but only implicitly, via the temperature gradient. This is a simplifying assumption that in many cases allows for an analytic evaluation of the pressure.

We shall consider three expressions that approximate the experimental data of saturated water vapor (in units of hPa). The first is a power-law expression with two adjusted parameters, hereafter referred to as PL2:

$$P_W^{\mathrm{sat}}(T) = \left(\frac{T}{247.1}\right)^{18.36}, \quad (26)$$

which has been used in this form by several authors.[4,9,10]

A physically more realistic expression is the Clausius–Clapeyron equation:

$$P_W^{\mathrm{sat}}(T) = \exp(a - b/T), \quad (27)$$

with $a = 21.39$ and $b = (m_W/k)L_{WD} = 5349\ \mathrm{K}^{-1}$, where L_{WD} is the latent evaporation heat in J/kmol, taken constant at its average value over the fit interval. In the following we shall refer to this two-component Clausius–Clapeyron fit as CC2.

The flexibility of the fit function is increased by allowing more powers of T in the exponential. Ciddor[15] finds that a good fit is obtained with

$$P_W^{\mathrm{sat}}(T) = \exp(AT^2 + BT + C + D/T), \quad (28)$$

with $A = 1.2378847\ 10^{-5}\ \mathrm{K}^{-2}$, $B = -1.9121316\ 10^{-5}\ \mathrm{K}^{-1}$, $C = 29.33194026$, and $D = -6.3431645\ 10^3$ K. This equation is still basically of the Clausius–Clapeyron form, and we refer to it as CC4.

Data are shown in Fig. 2, together with these fits. It is seen that the CC4 gives an excellent fit over the full temperature range of the data. The CC2, obtained from a fit to the data below 50 °C, describes the data equally well in this region. The PL2 curve does not follow the general shape of the vapor pressure and has been chosen to match the data in the temperature region where observations are most likely to be made.

In the following subsections we shall review ways to solve Eq. (25), both numerically and analytically. The latter differs slightly from the approach in the *Explanatory Supplement*, where the dependence of the acceleration of gravity on height has been neglected.

A. Finding the Pressures by Numerical Integration

Equation (25) is a first-order differential equation in P_D. The right-hand side is only nonvanishing in the troposphere, where it can be evaluated for each height. Hence, Eq. (25) can be solved by standard numerical techniques. We choose the fourth Runge–Kutta method. The integration is subject to the condition that for chosen total sea-level pressure, P_0, and temperature, T_0,

$$P_D(0) = P_0 - P_W(T_0) = P_0 - RH \times P_W^{\mathrm{sat}}(T_0). \quad (29)$$

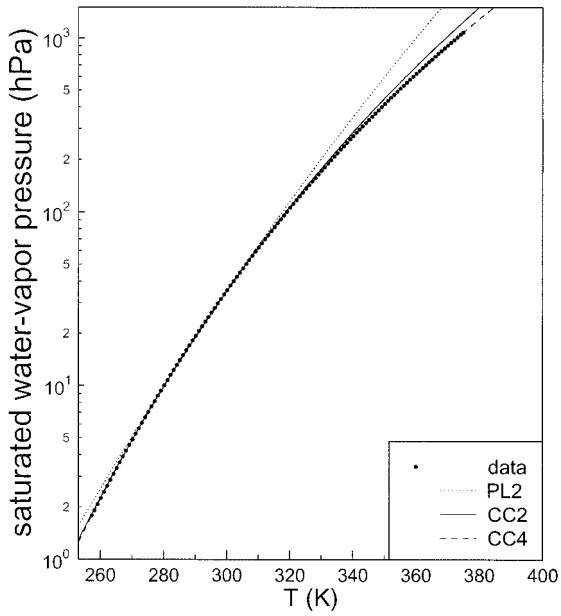

Fig. 2. Saturated vapor pressure of water. The data are from *The Handbook of Chemistry and Physics*.[3] The curves represent the different formula's: the power-law expression (PL2), the two- and four-parameter Clausius–Clapeyron forms CC2 and CC4, discussed in the text.

For later use $P_D(h)$ is then found by interpolation in a lookup table. $P_W(T)$ is found directly from its analytical expression, which is taken as either the PL2 form of Eq. (26), the CC2 form of Eq. (27), or the CC4 expression of Eq. (28).

B. Analytical Solutions for Dry Air

Numbering the seven different constant temperature-gradient intervals of the MUSA76 atmosphere by $j = 1$–7, and denoting by h_{1j} and T_{1j} the height and the temperature at the bottom of each interval, we introduce the following variables and constants:

$$h_j = h - h_{1j} \qquad \text{dim. m},$$

$$a_j = \frac{1}{T_{1j}}\left(\frac{\mathrm{d}T}{\mathrm{d}h}\right)_j \qquad \text{dim. m}^{-1},$$

$$c_j = \frac{m_D g(h_{1j})}{kT_{1j}} \qquad \text{dim. m}^{-1},$$

$$b_j = \frac{1}{R_E + h_{1j}} \qquad \text{dim. m}^{-1},$$

$$\eta_j = -\frac{a_j c_j}{(a_j - b_j)^2} \qquad \text{dimensionless},$$

$$\zeta_j = -\frac{b_j}{(a_j - b_j)} \qquad \text{dimensionless}.$$

For dry air the differential equation, Eq. (25), reduces to

$$\frac{1}{P(h_j)}\frac{\mathrm{d}P(h_j)}{\mathrm{d}h_j} = \frac{-c_j}{(1 + a_j h_j)(1 + b_j h_j)^2} \tag{30}$$

and has the solution

$$P(h_j) = P(h_j = 0)\left(\frac{1 + a_j h_j}{1 + b_j h_j}\right)^{\eta_j} \exp\left(-\frac{c_j \zeta_j h_j}{1 + b_j h_j}\right). \tag{31}$$

Note that these results reduce to the expressions given in the *Explanatory Supplement* when neglecting the dependence of the acceleration of gravity on height. Then, $b_j \to 0$, and $\eta_j \to -c_j/a_j \equiv \gamma_j$ and

$$P(h_j) = P(h_j = 0)\left[\frac{T(h_j)}{T_{1j}}\right]^{\gamma_j} \qquad (\text{if } a_j \neq 0), \tag{32}$$

$$P(h_j) = P(h_j = 0)\exp\left[-\frac{m_D g(h_{1j}) h_j}{kT_{1j}}\right] \qquad (\text{if } a_j = 0). \tag{33}$$

C. Analytical Solutions for the Water-Vapor Correction

The water-vapor correction is applied only for the troposphere. Equation (25) may be rewritten to a differential equation in T, making use of the dependence of temperature on height. The result is

$$\frac{\mathrm{d}P_D}{\mathrm{d}(T/T_0)} - \frac{\eta_D P_D}{T/T_0(1 - \zeta T/T_0)^2} = -\frac{\mathrm{d}P_W}{\mathrm{d}(T/T_0)} + \frac{\eta_W P_W}{T/T_0(1 - \zeta T/T_0)^2}, \tag{34}$$

where $\eta_W = (m_W/m_D)\eta_D$ and where we have dropped the index referring to the interval number, as we consider only the troposphere. The general solution of the homogeneous equation, with vanishing right-hand side is

$$P_D(T)(\text{hom.}) = C(T/T_0)^{\eta_D}(1 - \zeta)^{\eta_D} \exp\left(\frac{\eta_D}{1 - \zeta}\right) \times (1 - \zeta T/T_0)^{-\eta_D} \exp\left[-\frac{\eta_D}{1 - \zeta T/T_0}\right], \tag{35}$$

which also would follow from Eq. (31). It differs from the result of the *Explanatory Supplement* by the presence of the additional factor

$$Z(\eta_D, \zeta, T/T_0) \equiv (1 - \zeta)^{\eta_D} \exp\left(\frac{\eta_D}{1 - \zeta}\right) \times (1\zeta T/T_0)^{-\eta_D} \exp\left[-\frac{\eta_D}{1 - \zeta T/T_0}\right]. \tag{36}$$

Throughout the troposphere, with values $\eta_D = 5.1829$ and $\zeta = 0.0069255$, $Z(\eta_D, \zeta, T/T_0)$ never differs from unity by more than 10^{-4}. Neglecting the variation of gravitation with height means $\zeta \to 0$ and $Z(\eta_D, 0, T/T_0) = 1$ and with $\eta_D \to \gamma$, Eq. (35) reduces to the result of the *Explanatory Supplement*.

1. Water-Vapor Correction from the Power-Law Expression

To arrive at the general solution of the full Eq. (34), a special solution of it must be added to the above general solution of the homogeneous equation. In the *Explanatory Supplement*, this has been chosen to obey the same power-law expression as the saturated water-vapor expression itself:

$$P_D(T)(\text{spec.}) = DP_W(T) = DP_W(T_0)(T/T_0)^{\delta} \quad \text{with } P_W(T_0) = \text{RH}(T_0/247.1)^{\delta}, \quad (37)$$

with $\delta = 18.36$.

This does not allow for an obvious special solution of Eq. (34). Observing, however, that $Z(\delta, \zeta, T/T_0)$ differs from unity by no more than 3×10^{-4}, an equally good fit to the water-vapor pressure data in Fig. 2 is provided by

$$P_W(T) = \text{RH} \times (T_0/247.1)^{\delta}(T/T_0)^{\delta}Z(\delta, \zeta, T/T_0). \quad (38)$$

Then it follows that a full solution of Eq. (34) will have the form

$$P_D(T) = C(T/T_0)^{\eta_D}Z(\eta_D, \zeta, T/T_0) + D(T/T_0)^{\delta}Z(\delta, \zeta, T/T_0), \quad (39)$$

and the constants C and D follow from Eqs. (34) and (29):

$$D = P_W(T_0)\left(\frac{\eta_W - \delta}{\delta - \eta_D}\right), \quad (40)$$

$$C = P_0 - P_W(T_0) - D. \quad (41)$$

2. Water-Vapor Correction from the CC2 Clausius–Clapeyron Expression

Next we attempt to base the water-vapor correction on the Clausius–Clapeyron CC2 form, which fits the data over a much wider range. Thus, taking $P_W(T_0)$ from Eq. (27), we anticipate the full solution to be

$$P_D(T) = C(1 - \zeta)^{\eta_D}\exp\left(\frac{\eta_D}{1 - \zeta}\right) \times \left(\frac{T/T_0}{1 - \zeta T/T_0}\right)^{\eta_D}\exp\left[-\frac{\eta_D}{1 - \zeta T/T_0}\right] + f(T)P_W(T_0)\exp\left[b\left(\frac{1}{T_0} - \frac{1}{T}\right)\right]. \quad (42)$$

By inserting this special solution into Eq. (34), one finds that $f(T)$ must satisfy

$$\frac{df}{dT} = \left[\frac{\eta_D}{T(1 - \zeta T/T_0)^2} - \frac{b}{T^2}\right]f(T) + \left[\frac{\eta_W}{T(1 - \zeta T/T_0)^2} - \frac{b}{T^2}\right]. \quad (43)$$

For this equation an analytical solution for $f(T)$ is not obvious. If, however, we make the small approximation that we neglect here the variation of the gravitational acceleration and put $\zeta = 0$, the solution is

$$f(T) = -1 + \left(\frac{\eta_D - \eta_W}{\eta_D}\right){}_1F_1\left(1, \eta_D + 1; \frac{b}{T}\right), \quad (44)$$

where ${}_1F_1$ is the confluent hypergeometrical function. The general solution for P_D is therefore

$$P_D(T) = C(1 - \zeta)^{\eta_D}\exp\left(\frac{\eta_D}{1 - \zeta}\right) \times \left(\frac{T/T_0}{1 - \zeta T/T_0}\right)^{\eta_D}\exp\left[-\frac{\eta_D}{1 - \zeta T/T_0}\right] - \left[1 - \left(\frac{\eta_D - \eta_W}{\eta_D}\right){}_1F_1\left(1, \eta_D + 1; \frac{b}{T}\right)\right] \times P_W(T_0)\exp\left[b\left(\frac{1}{T_0} - \frac{1}{T}\right)\right]. \quad (45)$$

The constant C is found from Eq. (29) by inserting $T = T_0$:

$$C = P_0 - \left(\frac{\eta_D - \eta_W}{\eta_D}\right){}_1F_1\left(1, \eta_D + 1; \frac{b}{T_0}\right)P_W(T_0). \quad (46)$$

5. Index of Refraction, Curvature, and Discontinuities

In Section 4 the derivations of the partial pressures for dry air and for the water-vapor correction have been dealt with in some detail. These may be found either fully numerically or fully analytically. In the latter case it was found necessary to make minor adjustments to the water-vapor expression. By inspection of the results it follows that the analytical and the numerical methods give identical results. As an example, the refractions obtained at 0° apparent altitude (90° zenith angle), which will be discussed in Section 6, differ by less than 0.0001 arcmin, both for dry air and for moist air.

With the pressures determined by either of the two methods, the index of refraction is found as a function of height from Eq. (19). Its derivative and hence the curvature are found by differentiation, which must be done numerically if the numerical method was used to obtain the pressures and may be done analytically if they were obtained analytically.

The result for the US1976 standard atmosphere is shown in Fig. 3. Since the temperature profile has piecewise constant temperature gradients, it shows kinks at the border between two such intervals. The index of refraction has kinks at the same places, but the curvature, being proportional to the logarithmic derivative, $(1/n/)dn/dh$, becomes discontinuous. This necessitates some special care for integration steps that lead across the border between two intervals.

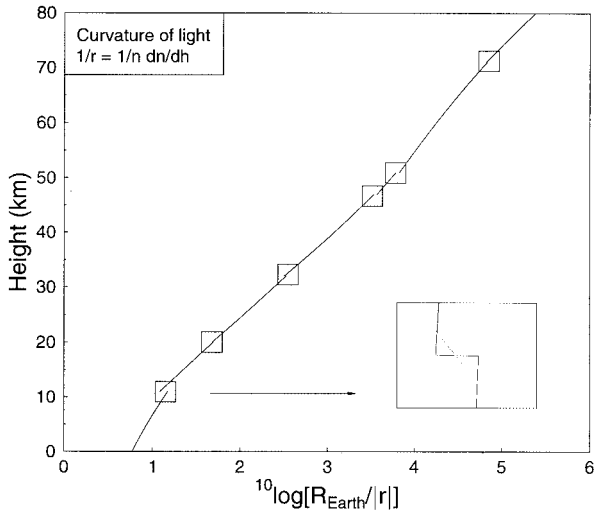

Fig. 3. Curvature, $1/r = (1/n)\mathrm{d}n/\mathrm{d}h$ in units of $1/R_{\mathrm{Earth}}$, of a locally horizontal ray for the US1976 standard atmosphere. The procedure to cope with the discontinuities, illustrated in the inset, is discussed in the text.

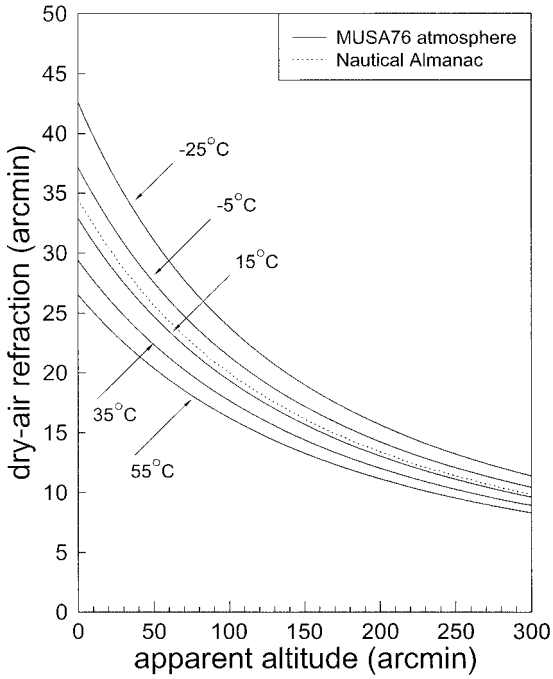

Fig. 4. Dry-air refractions for low apparent altitudes, calculated on the basis of the MUSA76 atmosphere for sea-level temperatures −25 °C, −5 °C, 15 °C (standard), 35 °C, and 55 °C. The sea-level pressure is 1013.25 hPa in all cases. The wavelength has been chosen as $\lambda = 0.574$ μm. For comparison the standard *Nautical Almanac* refraction is shown.

When evaluating the refraction integral, Eq. (16), one may conveniently split the integral into a sum over all intervals, finding the integration limits of each interval by use of Eq. (7). When doing full ray tracing, using numerical integration, one may similarly make an integration step end on the border between two intervals and let the next step begin there.

Another and easier way is to make the replacement

$$\frac{\mathrm{d}n}{\mathrm{d}h} \rightarrow \frac{27[n(h + \tfrac{1}{2}\Delta h) - n(h - \tfrac{1}{2}\Delta h)] - [n(h + \tfrac{3}{2}\Delta h) - n(h - \tfrac{3}{2}\Delta h)]}{24\Delta h}. \tag{47}$$

The expression at the right-hand side is exactly equal to the derivative when the latter is locally a polynomial of third order or less. It is therefore perfectly adequate to replace $\mathrm{d}n/\mathrm{d}h$ everywhere when the latter is continuous. However, across a discontinuity the replacement has the effect of smoothing as shown in the inset of Fig. 3. The effect of this replacement on the ray tracing may be judged best from its effect on the refraction integral, Eq. (16): the discontinuity is replaced with a smooth connection, *which does not change the integral across it*. When Δh is of the same order as the integration step size, the integrand does not now vary more violently than a third-order polynomial. Since the Runge–Kutta method is still exact for a fourth-order polynomial, it may now be applied without making extra provisions to let integration steps end precisely on the border between intervals. The same is true if one wishes to evaluate the refraction integral: There is no longer a need to split the integral into the separate contributions of the different intervals.

6. Results

In this section we present refractions for the MUSA76 atmosphere and study their dependence on sea-level temperature and pressure. We make a comparison of refractions obtained with the MUSA76 with those of the *Star Almanac*[1] and the *Nautical Almanac*.[2] In both cases we make a comparison with the Pulkovo tables.[6]

As pointed out at the end of Section 5, results do not depend on whether the pressures have been obtained by numerical integration or by their analytical expressions. The results presented in the following have been obtained with numerically determined pressures. Unless specified otherwise, a wavelength of 0.574 μm, conventionally chosen to represent mean star light, is used along with the CC4 expression of Eq. (28) for the water-vapor correction, when applicable.

A. Dry-Air Refractions for the MUSA76 Atmosphere

Refractions for low apparent altitude, for MUSA76 atmospheres of different sea-level temperatures and a fixed sea-level pressure of 1013.25 hPa, are shown

Table 2. US1976 Standard Atmosphere Refractions[a]

Zenith Ang. (deg)	Refraction (arcsec)	Zenith Ang. (deg)	Refraction (arcsec)
		72	173.93
5	5.00	74	196.49
10	10.07	76	225.00
15	15.31	78	262.20
20	20.79	80	312.78
25	26.64	81	345.52
30	32.98	82	385.34
35	39.98	83	434.68
40	47.90	84	497.25
45	57.07	85	578.72
50	67.98	86	688.25
55	81.40	87	841.19
60	98.62	88	1064.59
65	121.87	89	1408.82
70	155.61	90	1974.35

[a] P_0 = 1013.25 hPa, t_0 = 15 °C, 0% rel. humidity, lat. = 45°, λ = 0.574 μm, refractivity from Ref. 15.

in Fig. 4. A strong temperature dependence is evident. For comparison, the standard *Nautical Almanac* refraction,[2] meant for 10 °C and 1010 hPa, is shown. A more detailed comparison with the *Nautical Almanac* is given in a later subsection.

Refractions for the whole range of apparent altitudes are given in Table 2 for the US1976 atmosphere, i.e., for the standard choice of 15 °C and 1013.25 hPa.

It is sometimes desirable, given a tabulated standard refraction for (P_0, T_0), to make a quick estimate for the refraction at different pressure and temperature, (P_1, T_1). The *Nautical Almanac* has a special table for this purpose. The Pulkovo tables[6] give a relationship in the form of a scaling law,

$$\xi(P_1, T_1) = \left(\frac{P_1}{P_0}\right)^{\kappa}\left(\frac{T_0}{T_1}\right)^{\lambda}\xi(P_0, T_0), \qquad (48)$$

where λ and κ (which is the quantity A in the Pulkovo tables) depend on the angle of observation. While κ is close to unity for all observation angles, λ rises rapidly when approaching 0° apparent altitude.

We investigate this form for the MUSA76 atmosphere. In Fig. 5, panels (a) and (b), the scalings with pressure and temperature are investigated for the refractions at 0° apparent altitude. We find best values κ = 1.0856 and λ = 1.7081. This is close to the fourth edition of the Pulkovo tables,[17] which at 0° gives κ = 1.0859 and λ = 1.7046. In the fifth edition[6] κ has been made to depend also on pressure and is given as 1.0836 at 1000 hPa. Also, λ is given an

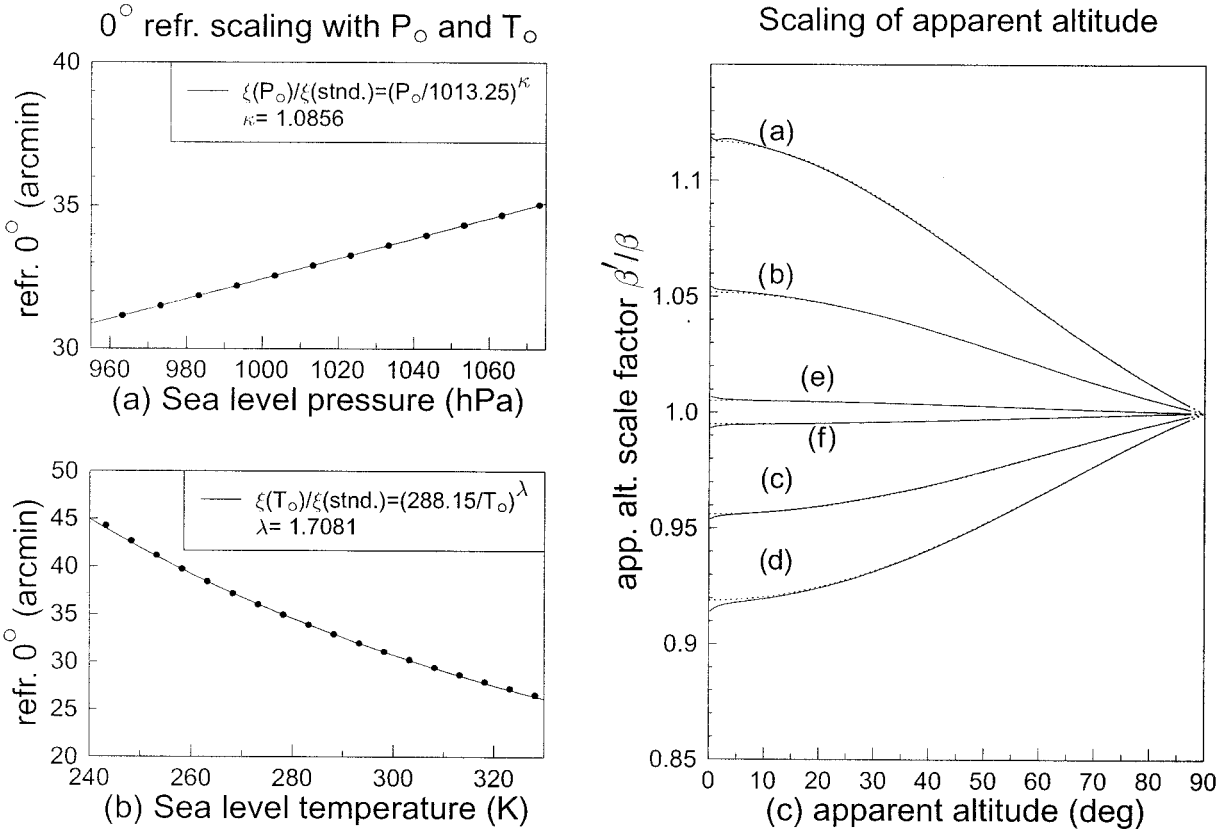

Fig. 5. (a) Dependence of the refraction at 0° apparent altitude on P_0, at T_0 = 288.15 °K. (b) Its dependence on T_0 at P_0 = 1013.25 hPa. (c) Apparent altitude scaling factors, relative to the standard T_0 = 288.15 °K, P_0 = 1013.25 hPa, for different sea-level temperatures and pressures: (a) t_0 = −25 °C, P_0 = 1013.25 hPa, (b) t_0 = −5 °C, P_0 = 1013.25 hPa, (c) t_0 = 35 °C, P_0 = 1013.25 hPa, (d) t_0 = 55 °C, P_0 = 1013.25 hPa, (e) t_0 = 15 °C, P_0 = 1073.25 hPa, (f) t_0 = 15 °C, P_0 = 953.25 hPa. The fits, discussed in the text, are shown as dashed curves.

additional dependence on temperature. Its value at 10 °C is 2.8053 for 0° apparent altitude.

This scaling does not come as a surprise: For normal atmospheres the radius of curvature of a light ray is approximately 5–7 times larger than the Earth's radius, and under these circumstances the refraction is basically the path integral of $\mathrm{d}n/\mathrm{d}h$ as follows from Eq. (16).

Most of the refraction is accumulated in the troposphere, where

$$\frac{\mathrm{d}n}{\mathrm{d}h} = -A_D \frac{P}{T^2}\left[\frac{\mathrm{d}T}{\mathrm{d}h} + B\right], \tag{49}$$

with $B \equiv m_D g/k = 3.4177\ 10^{-2}$ K/m. Hence, for low altitudes exponents not far from $\kappa \approx 1$ and $\lambda \approx 2$ should be expected to be adequate for Eq. (48), as indeed they are found.

Next we investigate the scaling at apparent altitudes, β, different from 0°. Without loss of generality one may put

$$\xi(P_1, T_1, \beta) = \left(\frac{P_1}{P_0}\right)^{\kappa}\left(\frac{T_0}{T_1}\right)^{\lambda} \xi(P_0, T_0, \beta'). \tag{50}$$

With the vertical scaling fixed at 0°, this means finding the ratio β'/β, by which the apparent altitude scale (horizontal) has to be compressed or decompressed. Panel (c) of Fig. 5 shows the results for different temperature–pressure combinations. It is clear from the figure that the altitude scaling is important and that its neglect is not justified.

We find that the altitude scaling can, with a high degree of accuracy, be described by

$$\tan(\beta') = \left(\frac{P_1}{P_0}\right)^{\mu}\left(\frac{T_0}{T_1}\right)^{\nu} \tan(\beta). \tag{51}$$

Fits are shown in Fig. 5(c). The values for μ and ν that give the best fits, vary little. Using the refractions from the US1976 atmosphere as a reference, from which refractions for a different temperature and pressure are to be estimated, we find as best average values $\mu = 0.087$ and $\nu = 0.690$.

Although we have obtained the exponents κ, λ, μ, and ν from independent fits, they are not uncorrelated: In the limit of large altitudes (small zenith angles), the refraction itself becomes to a very good approximation proportional to $(P/T)\tan^{-1}(\beta)$.[8,18] Hence, from Eqs. (50) and (51), one should have $\kappa \approx \mu + 1$ and $\lambda \approx \nu + 1$, which is found to be accurately fulfilled by the values that we derived above.

Thus we have arrived at a combined scaling for the MUSA76 refractions with sea-level pressure and temperature, expressed in Eqs. (50) and (51), that applies for all altitudes. It gives relative errors less than 5×10^{-3} for all altitudes, when applied for temperature shifts less than ±40 °C and even less than 1×10^{-3} for $\beta > 15°$ and a temperature shift of less than ±20 °C. The scaling with pressure induces no relative errors in excess of 1×10^{-4} for pressure shifts up to ±60 hPa.

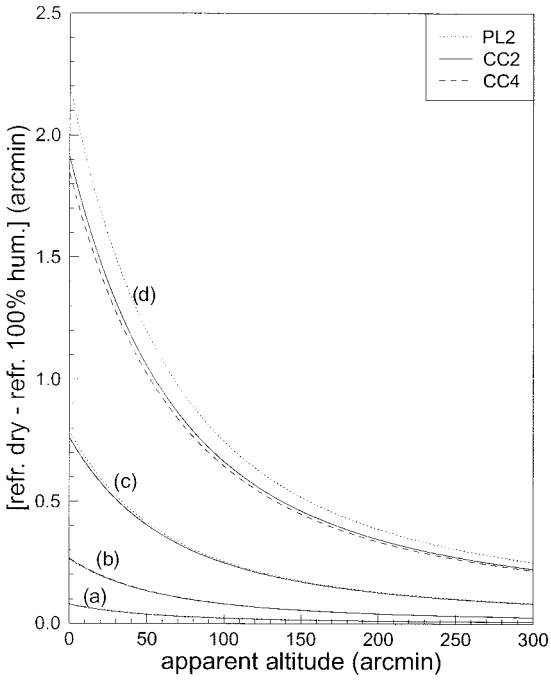

Fig. 6. Difference between refractions for dry air and for 100% humidity for the different equations for saturated water vapor, PL2, CC2 and CC4. The basis is the MUSA76 atmosphere for temperatures (a) −5 °C, (b) 15 °C (standard), (c) 35 °C, and (d) 55 °C at a sea-level pressure of 1013.25 hPa in all cases. λ = 0.574 μm.

B. Water-Vapor Correction

The MUSA76 refraction calculations of Subsection 6.A have been repeated, but now for a relative humidity of 100%. In Section 3 we discussed three different expressions for saturated water vapor, the power-law form, PL2 [Eq. (26)] and the two- and four-parameter Clausius–Clapeyron expressions, CC2 [Eq. (27)] and CC4 [Eq. (28)].

The difference between the dry-air and the moist-air refractions is shown in Fig. 6. There, the case for a ground temperature of −25 °C has been left out, as the difference was too small to be drawn. The water-vapor correction increases quickly with temperature. At 15 °C it is just below 0′.3, and the difference between the results for the three different water-vapor formulas may be neglected. At 35 °C the difference between the PL2 on the one hand and the CC2 and CC4 on the other becomes just noticeable. It is only at very extreme temperatures, such as 55 °C, that one sees a difference between the CC2 and the CC4 results. Of the three, the Clausius–Clapeyron expression CC4 gives the smaller contribution. Whenever one finds the difference important the Clausius–Clapeyron forms must be preferred over the power-law expression, because of their superior agreement with the data (Fig. 2).

C. Comparison for the *Star Almanac* Atmosphere

The *Star Almanac for Land Surveyors*[1] was first published in 1951. It gives refraction tables for zenith angles up to 80°, which are based on the tables of

Harzer from 1924.[19] The *Star Almanac* adopts a sea-level temperature of 7 °C and a sea-level pressure of 1005 hPa. The wavelength and the humidity are not specified.

Hohenkerk and Sinclair[9] have found that the *Star Almanac* refractions are closely reproduced under the following additional assumptions: The temperature lapse rate in the troposphere is -0.0065 K/m. From 11 km upwards the temperature is kept fixed. The wavelength is taken as $\lambda = 0.574$ μm and the relative humidity as 80%. The dry-air and water-vapor reduced refractivities are taken in the Cauchy forms, Eqs. (22) and (23). The following values for natural and geophysical constants are used:

$$R = Nk = 8314.36$$
(universal gas constant),
$$M_d = Nm_d = 28.966$$
(molar weight of dry air),
$$M_w = Nm_w = 18.016$$
(molar weight of water vapor),
$$R_{\text{Earth}} = 6{,}378{,}120 \text{ m}$$
(average radius of the Earth),
$$g = 9.784[1 - 0.0026 \cos(2\phi)]$$
(ϕ = obs. latitude).

The observer's latitude was chosen as 50°. The variation of the gravitational acceleration with height is neglected in the above formulation.

The calculations of Hohenkerk and Sinclair[9] use the refraction integral approach, discussed in Section 2, and were made for zenith angles from 10° to 80°. They find complete agreement with the *Star Almanac* tables, which give refractions in arcseconds, rounded to the nearest integer.

In the second column of Table 3 we present our calculations for the above specified *Star Almanac* atmosphere, for zenith angles from 5° to 90°. For all zenith angles, which are also given by Hohenkerk and Sinclair,[9] we find exactly the same values, till in the last decimal. Given this agreement, we may consider column 2 as representative for the *Star Almanac* atmosphere.

Columns 3–5 of Table 3 show the corresponding calculations for the MUSA76 atmosphere, with the sea-level temperature and pressure adjusted to the *Star Almanac* standards. For column 3 this is the only change: The reduced refractivities, A_D and A_W, are still in the forms of Eqs. (22) and (23), and the natural and geophysical constants are the same as in Ref. 9. The equivalent result for the Clausius–Clapeyron form CC2 [Eq. (27)] is given in column 4, where also the natural and geophysical constants of Ref. 3 have been adopted. Changing then only the CC2 water-vapor correction for CC4 gives the results of column 5. A comparison with the Pulkovo tables is made in column 6.

The differences between the values in columns 2–5 are very small. Yet, it is interesting to study the effect of a stepwise parameter change when going from the *Star Almanac* atmosphere to the MUSA76 atmosphere. This is shown in Table 4 for the refractions at 90° zenith angle.

We find that most of the changes have an effect of less than 1 arcsec. There are two exceptions: The different choice of the acceleration of gravity at sea level, embodied in $g(\phi)$, increases the refraction by 3 arcsec. It is compensated by the change in the mean radius of the Earth, which makes a 4-arcsec difference, but of opposite sign. The sum of the absolute values of all changes is nearly 10 arcsec, but it is by

Table 3. Comparison with the *Star Almanac* Atmosphere[a]

z (deg)	Star Alm.[b] (arcsec)	MUSA76[c] (arcsec)	MUSA76[d] (arcsec)	MUSA76[e] (arcsec)	Pulkovo[f] (arcsec)
5	5.10	5.10	5.09	5.09	5.09
10	10.27	10.27	10.27	10.27	10.26
15	15.60	15.60	15.60	15.60	15.60
20	21.19	21.19	21.19	21.19	21.18
25	27.15	27.15	27.15	27.15	27.14
30	33.61	33.61	33.61	33.61	33.59
35	40.76	40.76	40.75	40.75	40.74
40	48.83	48.83	48.82	48.82	48.80
45	58.17	58.17	58.16	58.16	58.14
50	69.29	69.29	69.28	69.28	69.26
55	82.98	82.98	82.97	82.97	82.94
60	100.53	100.53	100.51	100.51	100.48
65	124.25	124.24	124.22	124.22	124.18
70	158.66	158.65	158.63	158.63	158.57
75	214.03	214.01	213.98	213.98	213.91
80	319.18	319.15	319.10	319.10	319.03
85	591.90	591.80	591.71	591.71	592.03
90	2046.04	2045.16	2044.88	2044.80	2118.02

[a] $P_0 = 1005$ hPa, $t_0 = 7$ °C, 80% rel. humidity, $dT/dh = -0.0065$ K/m, lat. = 50° and $\lambda = 0.574$ μm.
[b] Recomputed *Star Almanac* values (this study and Ref. 9).
[c] Using $P_W^{\text{sat}} = (T/247.1)^{18.36}$ and $A_D(\lambda)$ and $A_W(\lambda)$ from Eqs. (22) and (23).
[d] Using the CC2 form for P_W^{sat}. $A_D(\lambda)^2$ and $A_W(\lambda)$ from Eqs. (21) and (24).
[e] Using the CC4 form for P_W^{sat}. $A_D(\lambda)$ and $A_W(\lambda)$ from Eqs. (21) and (24).
[f] Pulkovo refraction tables, 5th ed., 1985 (Ref. 6).

Table 4. Stepwise Change from *Star Almanac* to MUSA76

Parameter	Change from	Into	$\xi(z = 90°)$ (arcsec)	Atmosphere
—	—	—	2046.04	Star Alm.
Integration lim. (km)	80	85	2046.04	
R (J kmol^{-1} K^{-1})	8314.36	8314.472	2046.03	
M_D (kg)	28.966	28.964	2045.93	
R_E (m)	6378120	6356766	2041.88	
$g(0, \phi = 50°)$	9.78842	9.81065	2045.07	
$g(h)$	$g(h) = g(0)$	Eq. (18)	2044.18	
$P_W^{\text{sat}}(T)$	Eq. (26)	Eq. (28)	2044.07	
$A_W(\lambda)$	Eq. (23)	Eq. (24)	2044.30	
$A_D(\lambda)$	Eq. (22)	Eq. (21)	2043.83	
T-profile	Star Alm.	MUSA76	2044.80	MUSA76

cancellation of the different changes that the end results for the *Star Almanac* and for the MUSA76 atmosphere differ only by just over 1 arcsec.

The choice of the temperature profile deserves special attention. After all, this is the main feature that distinguishes the two atmospheres. The difference in refraction, when using one or the other, is just ~1 arcsec. But if we would shift the sea-level temperature downwards, from 7 to −10 °C, this difference would be more than 3 arcsec. The reason is that, in this example, the temperature profile of the upper part of the atmosphere is shifted together with that of the tropopause for the *Star Almanac* atmosphere, while for the MUSA76 atmosphere it is left unchanged and it is the height of the troposphere itself that is lowered. Hence, above the tropopause, the temperature profile of the *Star Almanac* is, in its entirity, lower than that of the MUSA76 atmosphere and progressively so, the lower one chooses the sea-level temperature.

The refractions from the Pulkovo tables (5th ed.), column 4 in Table 3, agree well with those for the *Star Almanac* and MUSA76 atmospheres up to a zenith angle of over 85°. In the last few degrees it increases considerably faster and gives a 74-arcsec larger refraction at the horizon. This difference can be traced back to the a difference in the low-altitude value of the temperature-scaling factor λ, which for the Pulkovo tables is quite different from that of the MUSA76 atmosphere, as discussed above.

D. Comparison for the *Nautical Almanac* Atmosphere

Since 1958, the year that the UK and the U.S. Nautical Almanacs became identical, the refraction tables have been the same as they are today. They are based on Garfinkel's theory[20] of 1944 and hence predate his second article of 1967.[21] The temperature profile on which they are based is similar to that of the *Star Almanac*, but for $t_0 = 10$ °C and $P_0 = 1010$ hPa. An important difference is the temperature lapse rate in the troposphere, which is taken as −0.005694 K/m. Garfinkel's 1944 study was based on an adopted refractive index at 0 °C and 1013.25 hPa of $n = 1.00029429$, which has been significantly improved since.

Hohenkerk and Sinclair[9] have recomputed some of the refractions, notably for large zenith angles, and find general, though not exact, agreement with Garfinkel's program.[21] To be consistent with the *Nautical Almanac* tables, they had to assume a wavelength of 0.50169 μm.

We have repeated these calculations with our own program. Again, as in the case of the *Star Almanac*, we find exact agreement with the results of Hohenkerk and Sinclair,[9] and we will use these results to represent the *Nautical Almanac* refractions. They are given in Table 5 in columns 2 and 3. In column 4 refractions based on the MUSA76 atmosphere are given, for λ = 0.574 μm, and the corresponding refractions from the Pulkovo tables are shown in column 5.

Contrary to the case in Subsection 6.C, where we studied the *Star Almanac*, the differences are large, especially for large zenith angles. The effect of choosing a different temperature lapse rate in the troposphere is found to be important. For $z = 90°$, the difference is more than 24 arcsec as seen from columns 1 and 2.

Using the same wavelength of 0.50169 μm, the MUSA76 atmosphere gives a refraction of 2039.32 at the horizon, close to the result for the *Nautical Almanac* atmosphere with a lapse rate of −0.0065 K/m. This is consistent with our previous comparison for the *Star Almanac*. Hence, the difference of the horizon refractions in columns 2 and 3 is almost entirely due to the different choice of the wavelength.

The agreement of the Pulkovo tables with the MUSA76 refractions is reasonable up to above 85° zenith angle. Its increase in the last few degrees is again much steeper. While at $z = 85°$ it gives the same refraction as the *Nautical Almanac*, it is some 20 arcsec higher at the horizon.

E. Refraction and Temperature Gradient

The temperature gradient in the troposphere is never really constant. Especially in the lowest few hundred meters it may deviate considerably from the mean value of −0.0065 K/m. Day–night changes and seasonal changes may cause a considerable variation in refraction at low altitudes. This has all been known for a long time. For an excellent review the reader is referred to the article of Fletcher,[22] in which the variability of low-altitude refractions is explained in terms of the temperature gradient near sea level.

We are now in the position to illustrate this effect

Table 5. Comparison with the *Nautical Almanac* Atmosphere[a]

z (deg)	Naut. Alm.[b] (arcsec)	NAO63[c] (arcsec)	MUSA76[d] (arcsec)	Pulkovo[e] (arcsec)
5	5.10	5.10	5.07	5.10
10	10.28	10.28	10.22	10.28
15	15.62	15.62	15.53	15.62
20	21.21	21.21	21.09	21.21
25	27.18	27.18	27.02	27.17
30	33.64	33.64	33.45	33.64
35	40.79	40.79	40.56	40.79
40	48.87	48.87	48.60	48.87
45	58.23	58.23	57.89	58.22
50	69.36	69.36	68.96	69.35
55	83.06	83.06	82.58	83.04
60	100.62	100.62	100.05	100.60
65	124.36	124.36	123.64	124.34
70	158.80	158.80	157.88	158.77
75	214.20	214.20	212.96	214.16
80	319.20	319.39	317.52	319.35
85	592.21	591.92	588.37	592.12
90	2065.77	2041.04	2027.07	2086.63

[a] $P_0 = 1010$ hPa, $T_0 = 10$ °C, 0% rel. humidity, lat. = 50°, $dT/dh = -0.005694$ K/m and λ = 0.50169 μm.
[b] Recomputed results, present study and Ref. 9.
[c] For $dT/dh = -0.0065$ K/m, present study and Ref. 9.
[d] With λ = 0.574 μm and $A_D(\lambda)$ from Eq. (21).
[e] Pulkovo refraction tables, 5th ed., 1985 (Ref. 6).

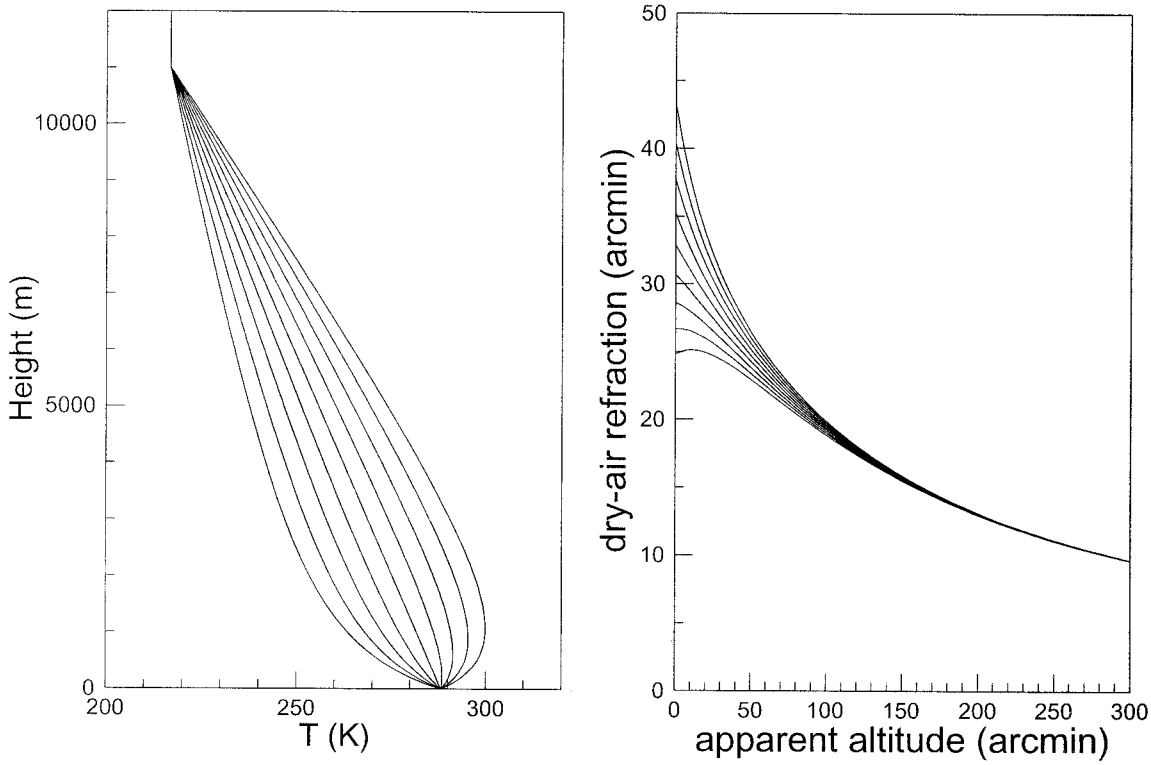

Fig. 7. Left, different temperature profiles in the troposphere for $P_0 = 1013.25$ hPa, $T_0 = 288.15$ K and temperature gradients, ranging (from left to right) from -0.0465 °C/m to 0.0335 °C/m in steps of 0.010 °C/m. The temperature profiles are obtained as in Eq. (52), with $H_C = 1$ km. Right, the corresponding dry-air refractions, increasing as the sea-level temperature gradient increases.

by means of ray-tracing calculations. In this subsection we study the effect of the temperature gradient on low-altitude refraction. To do this, we generalize the temperature profile in the troposphere by writing it as

$$T(h) = T_0 - 0.0065h + \left[\left(\frac{dT}{dh}\right)_0 + 0.0065\right] \times \left[\frac{h(H_T - h)}{H_T(1 + h/H_C)}\right], \quad (52)$$

where the final term is an addition to the standard temperature profile of the troposphere. The additional term vanishes at sea level, $h = 0$, and at the tropopause, $h = H_T$. Thus, the added temperature profile leaves intact the average temperature lapse rate in the troposphere, but at sea level the temperature gradient is now $(dT/dh)_0$. The parameter H_C determines the shape of the added temperature profile and gives roughly the height of the surface layer where the temperature gradient deviates from the troposphere average.

In Fig. 7, left panel, such temperature profiles are shown, for $t_0 = 15$ °C and 1013.25 hPa, the standard of the US1976 atmosphere. The sea-level temperature gradient is varied in steps of 0.010 K/m around the standard value of -0.0065 K/m. The parameter H_C has been set at 1000 m, confining the most drastic variation in temperature gradient to the lowest 2 km.

The effect on the refraction is shown in the right panel of Fig. 7. It must be compared with Fig. 4, where the effect of shifting the sea-level temperature is shown. One observes that shifting the sea-level temperature gradient, but not the temperature itself, has a very drastic effect, but only in the region of the lowest few degrees in apparent altitude.

There have been many attempts, in all times, to relate refractions, obtained by accurately timing the moment of sunset, with the predictions based on atmospheric models. This example shows that such studies are sensitive to the temperature gradient just above ground or sea level, rather than to the global features of the atmospheric model.

Especially when the moment of sunset is taken as the instant of a green flash, one should be careful. The green flash is normally not seen when the atmosphere is "standard," but its occurrence is usually associated with a nonstandard temperature gradient.[12]

7. Summary

We have studied the atmospheric refraction for the US1976 atmosphere, generalized to deal with arbitrary sea-level temperature and pressure. The so modified atmosphere has been named MUSA76. The presented method uses full ray tracing, based on the fourth-order Runge–Kutta method. The relation of the ray-tracing method to the usual evaluation the refraction integral is discussed in some detail.

Analytical and numerical procedures for evaluat-

ing, for a given temperature profile, the pressure at all heights are presented. Three different forms of the water-vapor correction are considered, first the usual power-law expression[4] and second the Clausius–Clapeyron forms with two and with four adjusted parameters.

Comparisons are made with the refractions of the *Star Almanac*, the *Nautical Almanac*, and the Pulkovo tables. Differences with the results from the MUSA76 atmosphere are discussed and their origins investigated.

A computer-based program, REF2001, for calculating refractions in the MUSA76 atmosphere as described in this paper, is available from the author.[23]

The author thanks Waldemar Lehn, Günther Können, and Catherine Hohenkerk for many useful discussions.

References

1. *The Star Almanac for Land Surveyors* (Her Majesty's Nautical Almanac Office, London, 1st ed., 1951).
2. *The Nautical Almanac* (Her Majesty's Nautical Almanac Office, London, and Nautical Almanac Office United States, Washington, D.C., 1st combined ed., 1958, printed yearly).
3. D. R. Lide, *Handbook of Chemistry and Physics*, 81st ed. (CRC Press, Boca Raton, Fla., 2000).
4. P. K. Seidelmann, ed., *Explanatory Supplement to the Astronomical Almanac* (University Science Books, Mill Valley, Calif., 1992).
5. L. H. Auer and E. M. Standish, "Astronomical refraction: computational method for all zenith angles," Astron. J. **119,** 2472–2477 (2000).
6. V. K. Balakin, ed., *Refraction Tables of the Pulkovo Observatory*, 5th ed. (Nauka, Leningrad, 1985).
7. M. Born and E. Wolf, *Principles of Optics*, 7th ed. (Cambridge University, Cambridge, UK, 1999).
8. W. M. Smart, *Textbook on Spherical Astronomy*, 6th ed. revised by R. M. Green (Cambridge University, Cambridge, UK, 1977).
9. C. Y. Hohenkerk and A. T. Sinclair, "The computation of angular atmospheric refraction at large zenith angles," NAO Tech. Note 63 (HM Nautical Almanac Office, Royal Greenwich Observatory, Greenwich, 1985).
10. A. T. Sinclair, "The effect of atmospheric refraction on laser ranging data," NAO Tech. Note 59 (HM Nautical Almanac Office, Royal Greenwich Observatory, Greenwich, 1982).
11. S. Y. van der Werf, G. P. Können, W. H. Lehn, F. Steenhuisen, and W. P. S. Davidson, "Gerrit de Veer's true and perfect description of the Novaya Zemlya effect, 24–27 January 1597," Appl. Opt. **42,** 379–389 (2003).
12. S. Y. van der Werf, G. P. Können, and W. H. Lehn, "Novaya Zemlya effect and sunsets," Appl. Opt. **42,** 367–378 (2003).
13. R. D. Sampson, E. P. Lozowski, and A. E. Peterson, "A comparison of modeled and observed astronomical refraction of the setting Sun," Appl. Opt. **42,** 342–353 (2003).
14. B. Edlen, "The refractive index of air," Metrologia **2,** 71–80 (1966).
15. P. E. Ciddor, "Refractive index of air: new equations for the visible and near infrared," Appl. Opt. **35,** 1566–1573 (1966).
16. J. C. Owen, "Optical refractive index of air: dependence on pressure, temperature, and composition," Appl. Opt. **6,** 51–59 (1967).
17. A. A. Michailov, ed., *Refraction Tables of the Pulkovo Observatory*, 4th ed. (Academy of Sciences Press, Moscow, Leningrad, 1956).
18. J. Saastamoinen, "Introduction to the practical computation of astronomical refraction," Bull. Geod. **106,** 383–397 (1972).
19. P. Harzer, "Gebrauchstabellen zur Berechnung der Ablenkungen der Lichtstrahlen in der Atmosphäre der Erden für die Beobachtungen am groszer Kieler Meridiankreise," Publikation der Sternwarte in Kiel **14** (1924).
20. B. Garfinkel, "An investigation in the theory of astronomical refraction," Astron. J. **50,** 169–179 (1944).
21. B. Garfinkel, "Astronomical refraction in a polytropic atmosphere," Astron. J. **72,** 235–254 (1967).
22. A. Fletcher, "Astronomical refraction at low altitudes in marine navigation," J. Inst. Navigation **5,** 307–330 (1952).
23. S. Y. van der Werf, Program REF2001, unpublished. Available from the author.